Korean J. Chem. Eng., **27**(1), 253-260 (2010)
DOI: 10.1007/s11814-009-0327-z

Water and mercaptan adsorption on 13X zeolite in natural gas purification process

Babak Shirani*, Tahereh Kaghazchi*,†, and Masoud Beheshti**

*Chemical Engineering Department, Amirkabir University of Technology, Tehran, Iran
**Chemical Engineering Department, Isfahan University, Isfahan, Iran
(*Received 3 June 2009 • accepted 6 July 2009*)

Abstract−The aim of this work is to model the adsorption process used for mercaptan and water removal from natural gas. Three fixed beds containing Zeolite molecular sieve type 13X, are used in this plant. In this operation, two beds are in process for adsorption purposes and the other one is regenerated simultaneously. This system is also operated under isothermal condition. In modeling of this process, rate of adsorption is approximated by linear driving force (LDF) expression, and the extended Langmuir isotherm is used to describe adsorption equilibrium. The set of partial differential equations of dynamic model is solved by Crank-Nicolson method. The effect of equations of state is also studied and the best equation fitting the industrial data is selected. Also, concentration profile is presented versus bed length at various times. The influences of pressure, inlet concentration and bed height on the breakthrough time are also investigated.

Key words: Adsorption, 13X Zeolite, Natural Gas, Multicomponent Separation, Modeling, Feed Effect

INTRODUCTION

Natural gas consists of many components and contains many impurities; two of the most important impurities are water and mercaptan. These two components cause several problems like corrosion, freezing, etc., in the gas industry, and in order to remove these components, several processes are used such as absorption, cryogenic distillation, adsorption, etc.

The adsorption process has been extensively used in the industry, for gas separation and purification. Compared with other separation processes, it is economically and technologically plausible. In this process some components of gas separate and adsorb on the surface of the adsorbents by chemical or physical adsorption. Physical adsorption of microporous materials has recently received more attention for gas separation and different kind of materials can also be used as adsorbent, like alumino silicate, silica gel, zeolite, etc. Zeolites are crystalline microporous structures with uniformly sized pores of molecular dimensions. The major advantages of using zeolites are their high ability for successive regeneration and high selectivity for adsorbing specific materials.

Two main technology of adsorption processes are temperature swing adsorption (TSA) and pressure swing adsorption (PSA). Processes operate between a low temperature level during adsorption and high temperature level during desorption and pressure swing adsorption (PSA). Processes work between a high pressure level during adsorption and a low pressure level during desorption [1].

To design adsorption processes, a better knowledge about how these processes work is needed. In the past, such beds were designed empirically through extensive experimentation process development units, so it was both expensive and time consuming [2]. Modeling and simulation of such processes improves process efficiency.

†To whom correspondence should be addressed.
E-mail: kaghazch@aut.ac.ir

Modeling and simulation of gas adsorption in a molecular sieve bed and also the mass and heat transfer studies are investigated by number of scientists. Mathias et al. [3] found adsorption isotherm of oxygen and nitrogen on the zeolite. Serbezov et al. [4] introduced a nonisothermal model for adsorption of air pollutant on the 5A zeolites. Gorbach et al. [5] performed some experimental data in the case of water vapor adsorption on the 4A zeolite and introduced its isotherm in the large area of water vapor pressure and temperature. Several workers examined the effect of operating parameters like the effect of velocity, operating temperature and pressure, feed concentration, etc. Details of these researches have been given by Ruthven et al. [6].

In this work, the TSA process uses 13X zeolite molecular sieves. 13X zeolites are available in pellet form with uniform pore size of 10A. These adsorbents are selective and have high affinity to adsorb both water and mercaptan. The adsorption characteristics of beds, such as pressure effect, bed height and operating time effects on the breakthrough time, were considered in this research. In addition, the effect of inlet concentration of both water and mercaptan on both breakthrough time and exit concentration was investigated. Also, by means of different kinds of equations of state (ideal gas low, Peng-Robinson (PR), Soave-Redlich-Kwong (SRK)), the effect of these equations on the exit concentration was surveyed, and the best equation which was well correlated by industrial data was chosen for the other parts.

DESCRIPTION OF PROCESS

This process consists of three parallel beds with 13X zeolite molecular sieves. A water jacket is set around each bed so the adsorption and desorption heat is removed and beds are worked as heat exchangers. In each cycle two beds are taken in the process and one bed is regenerated. Each cycle takes 18 hours, the adsorption process takes 12 hours, the regeneration process takes 5.5 hours,

Table 1. Characteristics of adsorbents and adsorption bed

Parameter	Unit	Values
Bed height, L	m	5.5
Bed diameter, d	m	2.5
Bed porosity, ε	(-)	0.34
Particle diameter, d_P	m	0.0026
Particle density, ρ_P	Kg/m^3	630
Bed temperature, T	K	295
Operating time, t_{cycle}	hr	12
Bed pressure, P	kPa	6400
Adsorbent internal porosity	%	~38
Adsorbent bulk dry density	g/mL	0.58-0.64
Adsorbent surface area	m2/g	~0.6
Adsorbent sorptive capacity	g/g (dry)	0.25-0.36

Table 2. Characteristics of feed gas to adsorbent bed

Parameter	Unit	Values
Gas flow rate	Kmol/sec	6.6469
Gas pressure	kPa	6400
Gas temperature	K	295
Gas molecular weight	(-)	18.91
Gas viscosity	cp	1.37×10^{-2}
Water mol fraction	(-)	1.84×10^{-3}
Mercaptan mol fraction	(-)	2.497×10^{-4}
Other component mol fractions	(-)	0.9879303

and for about half an hour beds are in rest. The characteristics of adsorbents and adsorption beds are listed in Table 1.

To reduce the amount of water to be adsorbed and therefore to minimize the required adsorption capacity of beds, the input gas is cooled in a gas-gas exchanger and then in wet gas chiller to 22 ºC. After the gas is flowed into the adsorption beds, most of the water and mercaptan are separated from it. The characteristics of feed gas to adsorbent beds are listed in Table 2. Although it seems that the mole fractions of water and mercaptan are low, these amounts are really high and undesirable for natural gas. The amounts of water and mercaptan in the natural gas must be, respectively, lower than 1 ppm and 20 ppm. So in order to reduce the amount of these two components, it is necessary to separate them from the gas.

A slip stream of dry gas exiting the beds is used as regeneration gas. The flow rate is set to 7% of the total feed gas flow to the dryer. This slip stream is heated to 300 ºC in the regeneration furnace (the design assumes a temperature drop of 20 ºC in the transfer line, so the regeneration gas temperature is 280 ºC entering the dryers) and passes through the regenerating molecular sieve bed contrary to feed gas direction.

The wet and hot effluent gas is cooled in the regeneration gas air cooler and the condensed water is removed in the regeneration gas separator. The recovered gas is then compressed in regeneration compressors and recycled back to gas-gas exchanger for cooling the gas feed flow. A flow diagram of the adsorption process is shown in Fig. 1 [7].

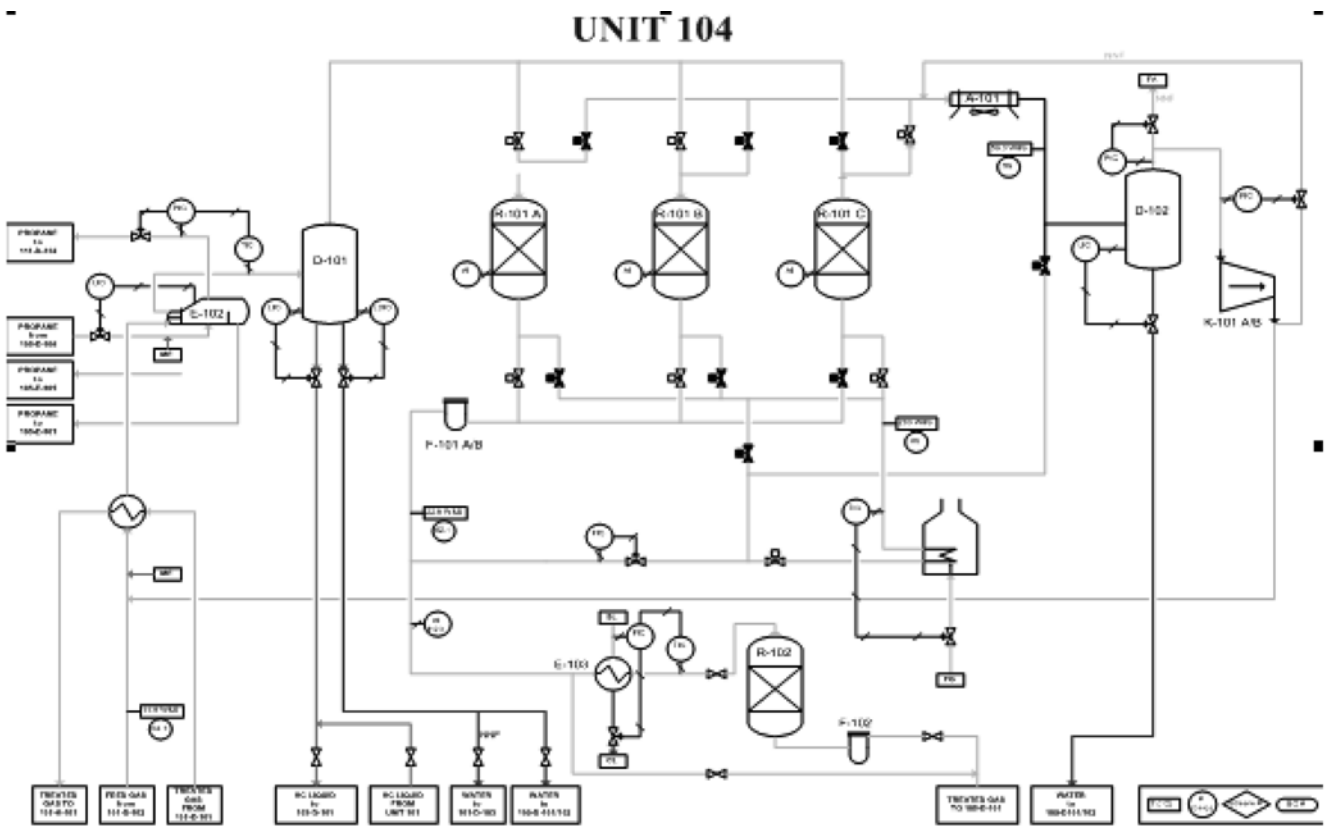

Fig. 1. Process flow diagram.

MATHEMATICAL MODELING

To understand the dynamic behaviors of adsorption beds, the mathematical models were developed on the basis of the following assumptions:

- The system operates under isothermal conditions. The temperature of the gas-wall heat transfer surface and the temperature within the particles are assumed to be homogeneous and constant (the inlet gas temperature is 22 °C and the outlet is 23 °C) and because of water jackets, the beds are working as a heat exchanger. According to Clause et al., the heat exchanger performances and modeling results are quite close to those of an isothermal operation [1]. Another reason for assuming isothermal operation is that the amount of water and mercaptan adsorbed is very low [8].
- The gradient of the concentration in the radial and angular direction is neglected (1D model). The assumption of neglecting radial gradient was widely accepted by numerous adsorption studies like Rota and Wankat [9], Jee et al. [10], and Kim et al. [11].
- Pressure drop along the bed length is negligible (about 70 kPa). According to Gupta et al. [12], the assumption of constant pressure derives from the fact that the concentration in the present study was very low (less than 1%).
- The fluid velocity throughout the bed is taken constant, because the amount of gas adsorbed is very small compared to the total flow entering the bed. Also there is a negligible pressure drop in the bed.
- The linear driving force model (LDF) is applied, using the overall diffusion coefficient of the boundary layer and diffusion within the porous particle.
- Thermal equilibrium between adsorbents and bulk flow is assumed.
- The flow pattern is described by the axially dispersed plug flow model.
- The equilibrium of adsorption is described by extended Langmuir isotherm.
- The gas behavior is described by three equations of state, ideal gas, PR and SRK.

1. Mass Balance in the Molecular Sieve Bed

Based on the preceding assumptions, the component mass balance for the bulk phase in the adsorption column is given by

$$\frac{\partial C_i}{\partial t} = -u\frac{\partial C_i}{\partial Z} + D_{ax}\frac{\partial^2 C_i}{\partial Z^2} - \frac{1-\varepsilon}{\varepsilon}\rho_P\frac{\partial q_i}{\partial t} \tag{1}$$

Where C_i and q_i are, respectively, concentration of components in the gas phase (Kmol/m^3) and in the adsorbed phase (Kmol/Kg), D_{ax} is the axial dispersion coefficient (m^2/s), u is the interstitial velocity (m/s), ρ_P is the bed's particle density (kg/m^3) and ε is the bed porosity. The value of D_{ax} is calculated through the following equation:

$$\frac{D_{ax,i}}{ud_p} = \gamma_1\frac{D_{m,i}}{ud_p} + \frac{1}{pe'_\infty\left(1+\beta\gamma_1\frac{D_{m,i}}{ud_p}\right)} \tag{2}$$

In Eq. (2), γ_1=0.73, β=13 and pe'_∞=2. D_{mi} is the molecular diffusivity and d_p is the particle's diameter.

The initial and boundary conditions for Eq. (1) are:

$$t=0 \qquad C_i=0 \tag{3}$$

$$t>0 \qquad Z=0 \qquad C_i=C_{iF} \tag{4}$$

$$Z=L \qquad \frac{\partial C_i}{\partial Z}=0 \tag{5}$$

Here only water and mercaptan are assumed to be adsorbed and other components are taken as non-adsorbing species (inert gas).

Referring to the assumptions, the linear driving force (LDF) model is used to describe the mass transfer rate of the gas and solid phases:

$$\frac{\partial q_i}{\partial t} = k_i(q_i^{sat} - q_i) \tag{6}$$

Where k_i is the mass transfer coefficient (s^{-1}), q_i^{sat} is the *i*th component concentration in the adsorbed phase in equilibrium with gas concentration (Kmol/Kg), and q_i is the mean concentration in the adsorbed phase.

Several correlations are used to estimate the value of k_i. According to Rodrigues et al. [13], when the adsorption time is too long the value of k_i is:

$$K_i = \frac{60D_{mi}}{d_p^2} \tag{7}$$

2. Adsorption Isotherm

There are several relations that describe the equilibrium of gas and adsorbent phases like Freundlich isotherm, Nitta isotherm, Langmuir isotherm, etc. In this work the extended Langmuir isotherm is used to predict the multicomponent adsorption equilibrium. This isotherm is suitable for gas adsorption [14] and could be easily developed for multicomponent adsorption systems. The equation is as follows:

$$\frac{q_i^{sat}}{q_{s,i}} = \frac{b_i p_i}{1+\sum_{i=1}^{nc} b_i p_i} \tag{8}$$

In the above equation p_i is the partial pressure (kPa), b_i and q_{si} are the *i*th component constant coefficients and q_{si} is the maximum adsorbed amount; b_i is a function of temperature as:

$$b_i = b_{oi}\exp\left(\frac{E_i}{RT}\right) \tag{9}$$

Where b_{oi} (1/kPa) and E_i (J/mol) are constants and vary for each component [15].

Gas feed consists of 22 components, but as mentioned earlier only water and mercaptan are assumed to be adsorbed and other components are treated as inert gas. Water and mercaptan adsorb on 13X zeolite more than other components because zeolite adsorbents have higher affinity to adsorb polar materials [16]. Also, by interaction of the permanent and large dipole moment of water with zeolite cation, the water affinity for adsorption is increased [17].

The extended Langmuir isotherm constant for adsorption of water and mercaptan in 13X zeolite is given in several papers. In this work the water isotherm is taken from Rege et al. [18] and because most of the mercaptan in the gas feed is ethyl mercaptan, so the isotherm data for mercaptan is taken from Weber et al. [19]. In this part, after curve fitting the data and putting them into the extended Langmuir isotherm, isotherm constants for these two components are obtained and shown in Table 3. These constants are dependent on temperature, and according to Rege et al., the water isotherm is

Table 3. Extended langmuir isotherm constants

	$q_{s,i}$ (kmol/kg)	b_{oi} (1/kPa)	E_i (J/mol)
Water	0.01234	1.112×10^{-5}	21297.64
Mercaptan	0.01187	1.672×10^{-5}	19060.18

obtained at 22 °C, which is the system temperature. The mercaptan isotherm is reported at 25 °C, which is in the vicinity of the system temperature.

3. Equations of State

Two equations of state (PR and SRK) and ideal gas law are used to relate the pressure of the system and the gas concentration, through the following equations:

$$\frac{P_t}{ZRT}=\sum_i C_i \tag{10}$$

$$P_i=y_iP_t=\frac{C_i}{\sum_i C_i}P_t \tag{11}$$

Combining 10 and 11 results in:

$$P_i=C_i\,ZRT \tag{12}$$

Where in the ideal gas equation Z=1 and in the two other equations, Z is calculated at the desired pressure and temperature. Because of their popularity, the equations of PR and SRK are not presented here and the details of these equations are available in the literature [20].

In this study the results of outlet concentrations of these equations are compared with the industrial data and the most suitable equation of state is used for modeling the process.

NUMERICAL SIMULATION METHOD

In this system, three kinds of equations (mass balance, mass transfer rate and extended Langmuir isotherm) must be solved at the same time. Because of the complexity and difficulty, these equations cannot be solved in analytical form, so numerical methods are chosen. Crank-Nicolson technique is used to solve these sets of equations. This technique is chosen because it has no limit for stability and can converge for a wide range of time and spatial discretization. With this method, differential equations are changed to algebraic equations and these equations then solved at the same time.

RESULTS AND DISCUSSION

1. Comparison of Equations of State

In this section the effect of two equations of state and ideal gas law on the exit concentration, is investigated. These equations are solved with the other equations of system (mass balance, mass transfer rate and Langmuir isotherm). The mole fractions of water and mercaptan in the gas phase, obtained by the model, are compared to industrial data at three points of the bed (inlet, outlet and in the middle of the bed) at the end of the operating time (12 hr). These data are obtained by sampling the gas flow at three points of the bed.

Fig. 2 shows water and mercaptan mole fraction in the gas phase against the bed length. As shown in this figure, for both water and

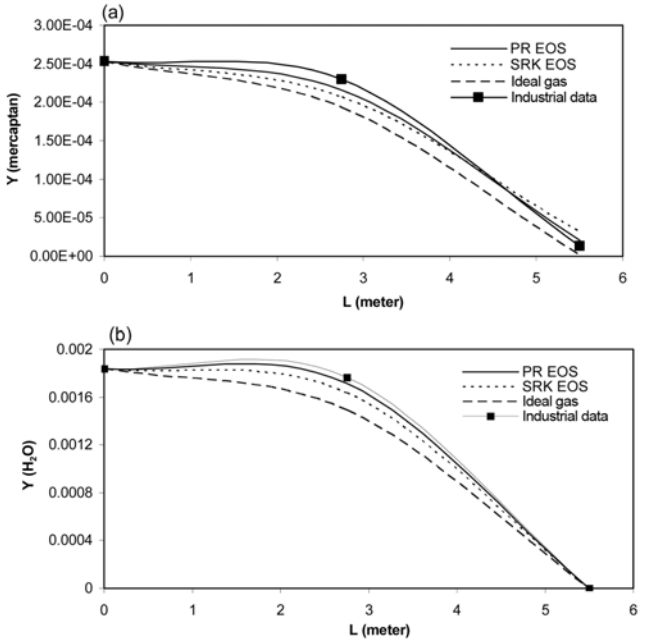

Fig. 2. Effect of equations of state on the (a) mercaptan, (b) water, gas phase mole fraction through the bed.

mercaptan PR EOS gives more accurate results than the two others. The results of SRK EOS are fairly good, but the ideal gas law's results do not have good accuracy with the industrial data, because the gas contains heavy and polar components. So assuming ideal behavior cannot be correct.

As an example, in the case of water, the outlet gas composition in the industrial sample is 1PPM and by using PR EOS, the model's result is 1.16 ppm. But the ideal gas law's and SRK's results are 0.01 ppm and 0.6 ppm, respectively, which are too far from industrial data.

According to the above discussion, PR EOS is selected as the equation to link the pressure and the concentration in the other parts of this study.

2. Adsorption Breakthrough Curves

In this part, as shown by Figs. 3 and 4, the simulation results are discussed. Figs. 3(a) and 3(b) are the adsorption breakthrough curves which demonstrate the relation between C/C_o ratio (outlet gas component concentration to inlet gas component concentration) and the length of the bed. These graphs show the mass transfer zone for four determinate times (t=1, 4, 8, 12 hr) in the bed. For water and mercaptan, since adsorption takes place, the ratio of C/C_o decreases as it passes through the bed.

Figs. 4(a) and 4(b) also show the breakthrough curve and it shows the relation between C/C_o ratio and the operating time. Here the concentration profile is displayed in four parts of bed (x=1/4L, 1/2L, 3/4L, L) and as expected, the concentration ratio increases with time until the adsorption saturation point is reached.

As shown in these graphs the mass transfer zone is proceeding through the bed, and finally it reaches the end of the bed. It can be seen from the graphs that the breakthrough curves for water are steeper than for mercaptan, and the reason is that water is adsorbed more than mercaptan and it reaches a saturation point with a higher velocity

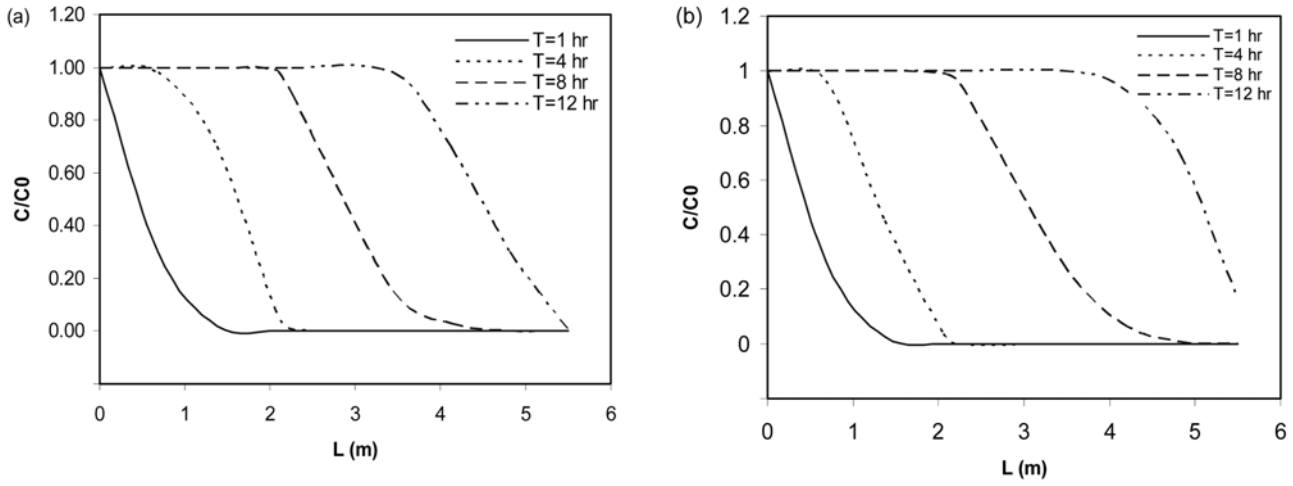

Fig. 3. (a) Water (b) mercaptan concentration ratio profile along the bed at different time.

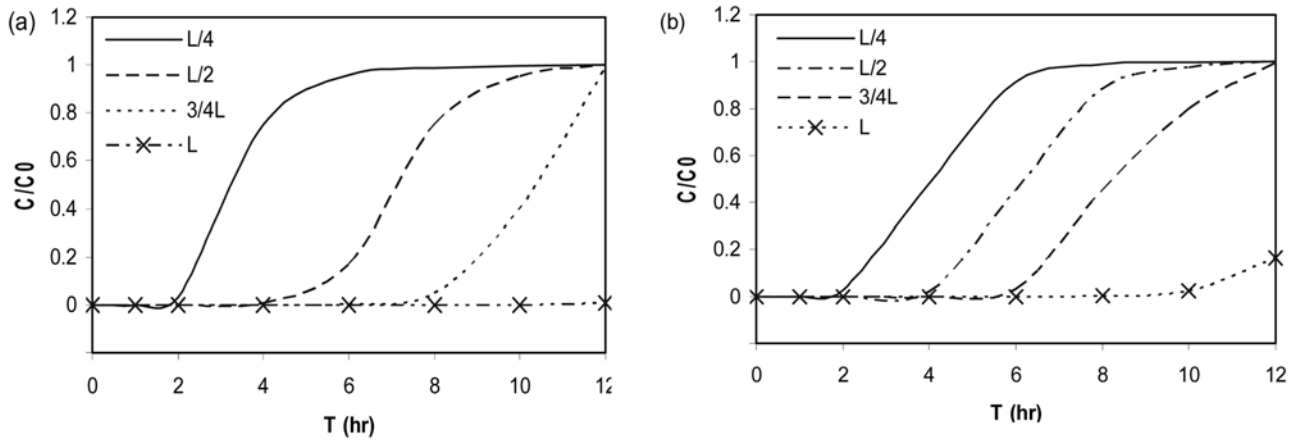

Fig. 4. (a) Water (b) mercaptan concentration ratio profile as a function of time in different parts of the bed.

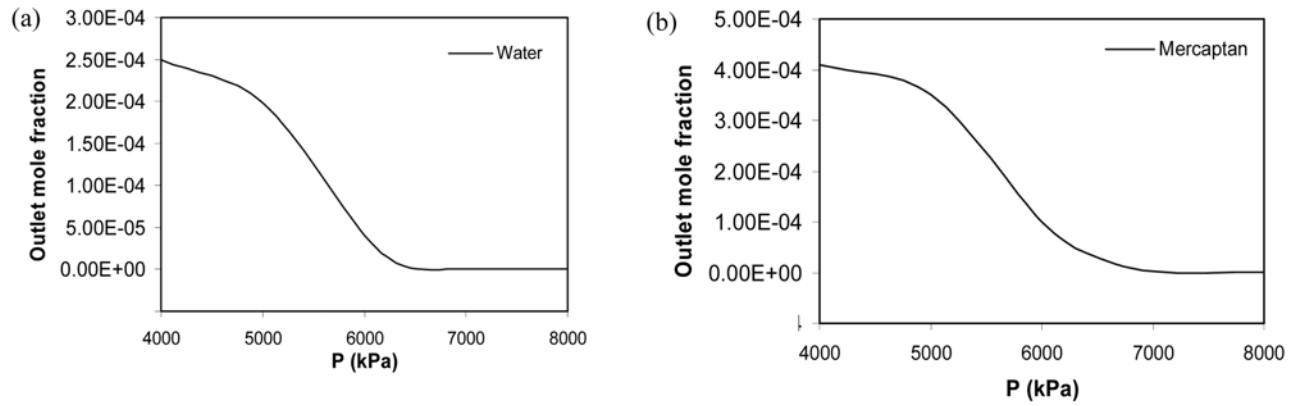

Fig. 5. Effect of pressure on the outlet concentration of (a) water (b) mercaptan at the end of the operating time.

than mercaptan.

3. Effect of Operating Pressure

The results in previous sections are obtained with the operating pressure of 6,400 kPa, but in this part the effect of operating pressure is seen on both breakthrough time and water and mercaptan outlet mole fractions. Fig. 5 shows the effect of pressure on the outlet mole fraction at the end of the operating time. As expected, the exit mole fractions decrease with pressure increase, and at high pressures, the values of exit concentrations are nearly zero. The reason for this phenomenon is that the adsorption operations mostly take place at high pressures and low temperatures.

In this study the breakthrough (C_B/C_o) point is set at 0.05. The

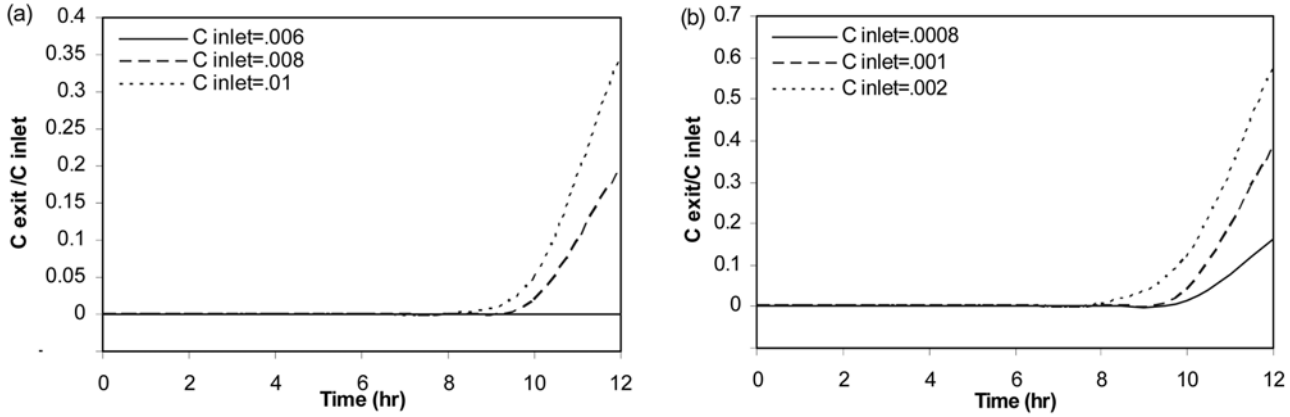

Fig. 6. Influence of (a) water (b) mercaptan inlet concentrations on the breakthrough curve and exit concentration.

value of breakthrough time for water at 6,400 kPa is 12.65 hr, and as mentioned above with pressure rise, the adsorption rate and consequently the breakthrough time are increased. Therefore for the case of water when the operating pressure is set to 8,500 kPa, the value of t_b (breakthrough time) is set to 14.1 hr, and when the pressure is reduced to 5,000 kPa, breakthrough time is 11.1 hr. Breakthrough time values for mercaptan at the pressures of 5,000, 6,400, 8,500 kPa are 11, 11.65, 12.3 hr, respectively. So the same results as water are obtained for mercaptan.

The above results establish the fact that increasing the pressure causes improvement in adsorption process, but due to some limitations, the pressure could not be increased much. One of these limitations is economical issues that happen at high operating pressures, like increasing the operating costs by means of using a larger compressor or special kinds of valves. Another reason is that the system and especially the beds can tolerate a certain pressure change. Therefore, for selecting a pressure as an operating pressure, many parameters must be considered.

4. Effect of Inlet Concentration

The effect of inlet adsorbate concentration on the effluent concentration is surveyed by using the model for various inlet concentrations of water and mercaptan. During this simulation other parameters such as pressure, bed height, operating time, etc. are kept constant.

Fig. 6 shows the outlet breakthrough curves for water and mercaptan at several input concentrations. As observed from these two graphs, the breakthrough time decreases when the inlet concentrations increase and breakthrough curves become much steeper.

In the case of water when C_o=0.006 kmol/m^3 the value of breakthrough time is t_b=12.65 hr. For the other two concentrations (C_o= 0.008 and C_o=0.01 kmol/m^3) the quantities of t_b are 10.5 hr and 9.95 hr, respectively.

Mercaptan also presents the same results as water, and when the inlet concentrations increase by C_o=0.0008, 0.001, 0.002 kmol/m^3 the values of breakthrough time decrease as t_b=10.7 hr, 10.1 hr, 9.3 hr.

The explanation for this phenomenon is that at high concentration, the driving force between the gas phase and adsorbent phase increases; thus equilibrium is reached faster. As a result, under this condition the adsorption rate and the amount adsorbed increase.

It should be mentioned that the model considers adsorption of both water and mercaptan and solves the related equations for both components at the same time. Therefore, the variations in the inlet concentration of one component affect the outlet concentration of the other component. This result is absolutely true in the real situation, because when the amount of one component increases, the adsorption rate for that component also increases. In this situation

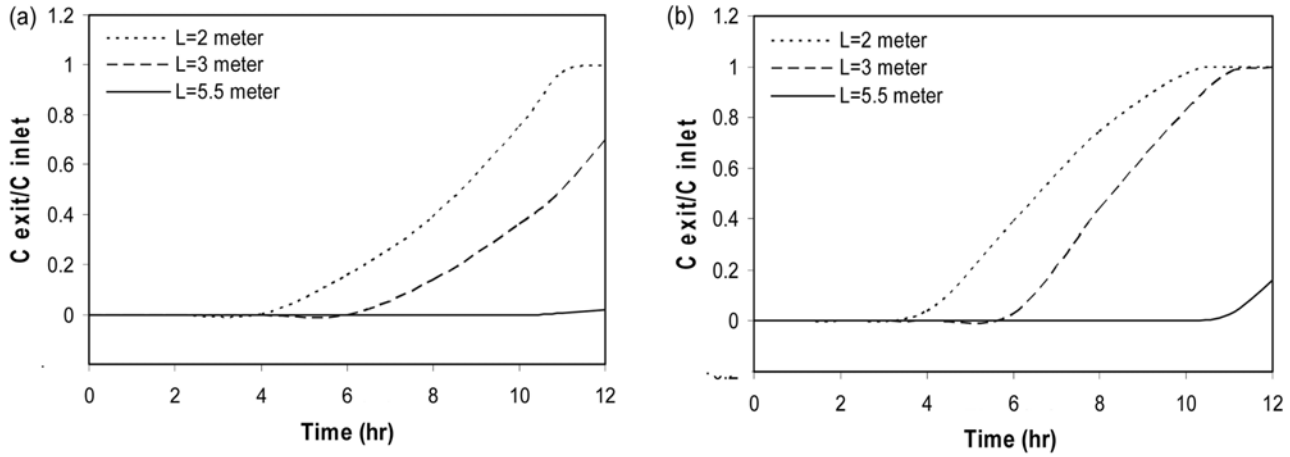

Fig. 7. Influence of bed height on the breakthrough curve and breakthrough time of (a) water (b) mercaptan.

the vacant pores for adsorbing the other components become fewer, so the outlet concentration of the second component increases. In this system because of the low adsorbate concentrations, the effect of one component adsorption on other component adsorption is not significant and can be neglected.

5. Effect of Bed Height

Effect of bed height is investigated by its influence on breakthrough time. Fig. 7 shows the outlet concentration of water and mercaptan as a function of operating time for several values of bed height.

Considering this figure for both water and mercaptan, it is apparent that as the bed height increases, the breakpoint time increases. For example, in the case of water when the bed's height is 5.5 meter (real situation) the breakpoint time is 11.2 hour, but when the length of the bed is decreased to 3 and 2 meters, the value of the breakpoint time is changed to 6.2 and 4.1 hr.

Another result from this figure is that as the bed height decreases, the outlet adsorbate concentration increases. Also, smaller beds are saturated more rapidly than larger ones, because smaller beds contain less adsorbent, and therefore the capacity of beds is much lower. Finally, the rate of adsorption is increased with decreasing the bed height.

Fig. 8 shows the relation between breakthrough time and bed height. As observed, with a good approximation, there is a linear relation between these two parameters, and also the above results can be deduced. The equation between breakthrough time and bed height is as follows:

$$b_t = A + B \times L \quad (13)$$

Where b_t is breakthrough time (hr), L is bed height (m) and A and B are constants for each component. The values of A and B for water and mercaptan are given in Table 4.

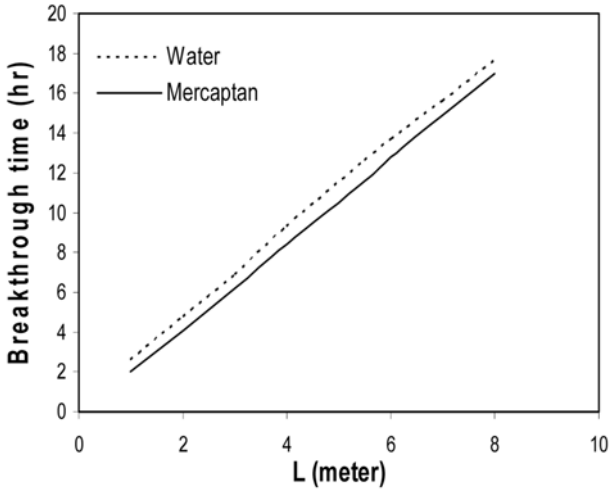

Fig. 8. Effect of bed height on the breakthrough time for water and mercaptan.

Table 4. Constants of Eq. (13)

Component	A	B
Water	0.4899	2.1734
Mercaptan	−0.1996	2.1533

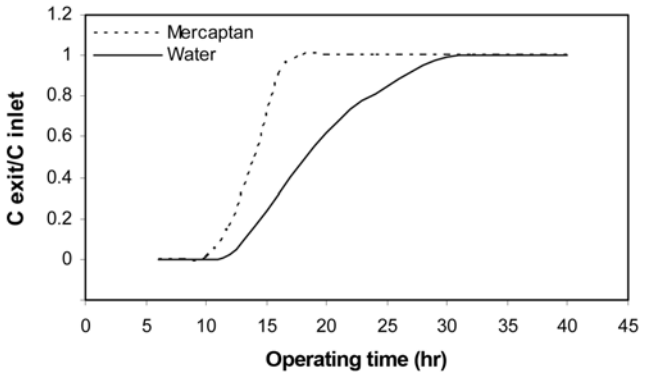

Fig. 9. Effect of operating time on the breakthrough curve for water and mercaptan.

6. Effect of Operating Time

The influence of the operating time on the outlet concentration is contrary to the effect of bed height. That is, when the operating time is increased, the outlet concentration (gas concentration at the end of the operating time) increases until it reaches the inlet concentration. At this time the bed is saturated, so adsorption does not take place.

In this system, the equilibrium of water and mercaptan is obtained at t_w=30 hr and t_M=18 hr. Because mercaptan is more polar and heavier than water, the adsorption rate of this component is higher than water's, and therefore it reaches equilibrium concentration more rapidly. Fig. 9 shows the concentration ratio (outlet concentration at the end of the operating time to inlet concentration) against the operating time. In this figure, as mentioned above, the mercaptan breakthrough curve is steeper and reaches equilibrium concentration much faster than water.

Operating time in this process is set to 12 hr. This time seemed to be the best time for operation, because at this time the ratio of inlet to outlet concentration of water is 6.3×10^{-4} and if the operating time is increased to 12.5 hr, then the concentration ratio becomes 0.02. As observed, this ratio increases considerably by about half an hour, and therefore choosing an operating time of more than 12 hr would not be appropriate.

CONCLUSIONS

Adsorption dynamics of a natural gas system (containing water, mercaptan, etc.) was studied by using separation beds, with TSA process, which were packed with 13X zeolite.

To increase the accuracy of the model, the effect of equations of state on the gas concentration was investigated and the results were compared to industrial data. In this system, ideal gas law results deviated from industrial data, but PR EOS fitted the industrial data with good approximation.

Effect of operating pressure was investigated and as observed, the outlet gas concentration decreased when the pressure increased.

For this system the effect of inlet concentration on the effluent concentration was obtained. Here with increasing the inlet concentration, the breakthrough curve becomes steeper and the breakthrough time was achieved sooner; therefore, the adsorption rate increased.

Influence of bed height on the breakthrough time was also studied and the results show that as it increased, the breakthrough time was increased. In this part a linear relationship between bed height and operating time was deduced. As a conclusion, at smaller bed height the effluent adsorption concentration increased more rapidly than for higher bed height.

The effect of operating time was also considered, and as a result, increasing the operating time caused an increase in the outlet concentration (at the end of the operating time).

In this work, the extended Langmuir isotherm was used to describe the equilibrium between gas and adsorbent phases, but numbers of other isotherms could be used in the modeling of gas adsorption. Investigating the influence of different isotherms on the model results, and choosing the best isotherm for this system will be the subject of a forthcoming study.

NOMENCLATURE

C : concentration in gas phase [Kmol/m^3]
q : concentration in adsorbed phase [Kmol/m^3]
D_{ax} : axial dispersion coefficient [m^2/s]
u : interstitial velocity [m/s]
t : time [hr]
z : zxial coordinate [m]
L : bed height [m]
d : bed diameter [m]
d_P : particle diameter [m]
T : bed temperature [°K]
P : bed pressure [kPa]
t_{cycle} : operating time [hr]
K_i : mass transfer coefficient [s^{-1}]
q^{sat} : equilibrium concentration [Kmol/kg]
D_m : molecular diffusivity [m^2/s]
b : langmuir isotherm parameter [1/kPa]
b_o : constant parameter in Eq. (9)
E : heat of adsorption [J/mol]
Z : compressibility factor
b_t : breakthrough time [hr]
A, B : parameters in Eq. (13)

Greek Letters

ρ_p : particle density [kg/m^3]
ε : bed porosity

REFERENCES

1. M. Clausse, J. Bonjour and F. Meunier, *Chem. Eng. Sci.*, **59**, 3657 (2004).
2. B. Sankararao and S. K. Gupta, *Comput. & Chem. Eng.*, **31**, 1282 (2007).
3. P. M. Mathias, R. Kumar, J. D. Moyer, J. M. S. Chork, S. R. Srinivasan, S. R. Auvil and O. Talu, *Ind. Eng. Chem. Res.*, **35**, 2477 (1996).
4. A. Serbezov and S. V. Sotirchos, *Adsorption*, **4**, 93 (1998).
5. A. Gorbach, M. Stegmaier and G. Eigenberger, *Adsorption*, **10**, 29 (2004).
6. D. M. Ruthven, *Principles of adsorption and adsorption processes*, Wiley, New York (1984).
7. Operating Manual, Document No. DB 2017 999 P312 202, SPGC Co.
8. C. A. Grande and A. E. Rodrigues, *Chem. Eng. Res. Des.*, **82**, 1604 (2004).
9. R. Rota and P. C. Wanket, *AIChE J.*, **36**, 1299 (1990).
10. J. G. Jee, H. Park, S. Haam and C.-H. Lee, *Ind. Chem. Res.*, **41**, 4383 (2002).
11. M.-B. Kim, J.-H. Moon, C.-H. Lee, M. Oh and W. Cho, *Korean J. Chem. Eng.*, **21**, 703 (2004).
12. A. Gupta, V. Gaur and N. Verma, *Chem. Eng. Process.*, **43**, 9 (2004).
13. A. E. Radrigues and M. M. Dias, *Chem. Eng. Sci.*, **37**, 489 (1998).
14. S. Sohn and D. Kim, *Chemosphere*, **58**, 115 (2005).
15. D. D. Do, *Adsorption analysis: Equilibria and kinetics*, Imperial College Press, London (1998).
16. J. H. Park, J. N. Kim, S. H. Cho, J. D. Kim and R. T. Yang, *Chem. Eng. Sci.*, **53**, 3951 (1998).
17. S. Auerbach, K. Carrado and P. Dutta, *Handbook of zeolite science & technology*, Marcel Dekker Inc., New York (2003).
18. S. U. Rege, R. T. Yang and M. A. Buzanowski, *Chem. Eng. Sci.*, **55**, 4827 (2000).
19. G. Weber, F. Benoit, J. P. Bellat, C. Paulin, P. Mougin and M. Thomas, *Micropor. Mesopor. Mater.*, **109**, 184 (2008).
20. S. M. Walas, *Phase equilibria in chemical engineering*, Butterworth Publishers (1985).